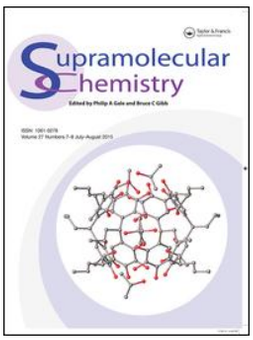

Supramolecular Chemistry

ISSN: 1061-0278 (Print) 1029-0478 (Online) Journal homepage: http://www.tandfonline.com/loi/gsch20

Cyclohexyl-diimine capped lower rim 1,3-di-derivatized calix[4]arene conjugate as sensor for Al^{3+} by spectroscopy, microscopy, titration calorimetry and DFT computations

Anita Nehra, Deepthi S. Yarramala, Sateesh Bandaru & Chebrolu Pulla Rao

To cite this article: Anita Nehra, Deepthi S. Yarramala, Sateesh Bandaru & Chebrolu Pulla Rao (2018): Cyclohexyl-diimine capped lower rim 1,3-di-derivatized calix[4]arene conjugate as sensor for Al^{3+} by spectroscopy, microscopy, titration calorimetry and DFT computations, Supramolecular Chemistry, DOI: 10.1080/10610278.2018.1424851

To link to this article: https://doi.org/10.1080/10610278.2018.1424851

Published online: 12 Jan 2018.

SUPRAMOLECULAR CHEMISTRY, 2018
https://doi.org/10.1080/10610278.2018.1424851

Taylor & Francis
Taylor & Francis Group

Cyclohexyl-diimine capped lower rim 1,3-di-derivatized calix[4]arene conjugate as sensor for Al^{3+} by spectroscopy, microscopy, titration calorimetry and DFT computations

Anita Nehra[a], Deepthi S. Yarramala[a], Sateesh Bandaru[b] and Chebrolu Pulla Rao[a]

[a]Bioinorganic Laboratory, Department of Chemistry, Indian Institute of Technology Bombay, Mumbai, India; [b]Algorithms Division, Beijing Computational Science Research Center, Beijing, China

ABSTRACT

A cyclohexane-*trans*-1,2-diimine capped conjugate of 1,3-calix[4]arene (**L**) has been synthesized and characterized using different analytical and spectral techniques. **L** has been shown to be sensitive toward Al^{3+} by exhibiting ~45-fold enhancement in its emission intensity at 445 nm upon complexation. All the other 15 metal ions showed almost no or minimal change in the fluorescence intensity of the **L** supporting that none of those 15 ions is sensed by **L**. The complexation between **L** and Al^{3+} has been further confirmed by absorption spectroscopy, isothermal titration calorimetry and ESI MS. The isotopic peak pattern of the ESI MS peak clearly confirmed the presence of aluminum in the 1:1 complex formed. The need for the flexible cap moiety for bringing selectivity to Al^{3+} was proven by comparing the titration studies with the corresponding control molecules. The sensing of Al^{3+} by **L** in the solid powder was demonstrated by fluorescence microscopy. The supramolecular behavior of **L** changes from simple spherical type morphology in **L** to an aggregated micro pots and fibers upon Al^{3+} binding. The DFT computational study yielded a distorted tetrahedral complex of the dianionic receptor resulting in AlN_2O_2 core.

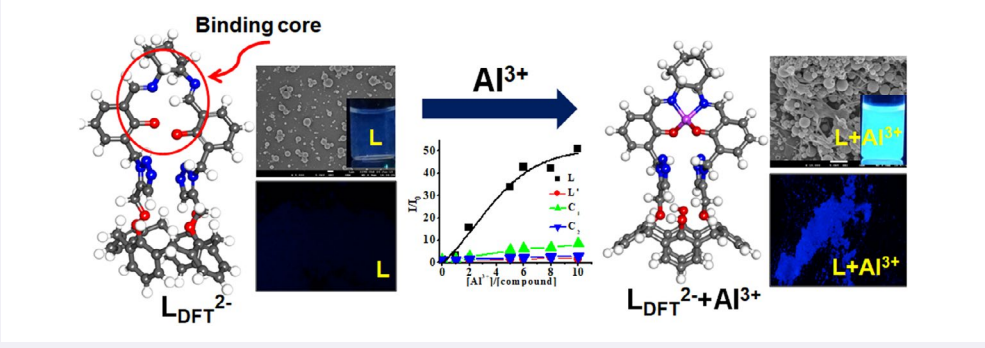

ARTICLE HISTORY
Received 29 November 2017
Accepted 3 January 2018

KEYWORDS
Receptor for Al^{3+}; cyclohexyl-diimine capped lower rim 1; 3-di-calix[4]arene conjugate; scanning electron microscopy (SEM); isothermal titration calorimetry (ITC); DFT computational study

Introduction

The development of a chemosensor for selective recognition of one of the earth's most abundant metal ion, *viz.*, Al^{3+} is of prime interest (*1–11*). Aluminum is a widely used metal in daily life, as food additive, as surgery materials, and in medicines, cosmetics and packaging because of its stable physical and chemical properties (*12–14*). Excess of Al^{3+} in blood may cause neurodegenerative disorders like Parkinson's and Alzheimer's diseases (*15–19*). Therefore, the detection of Al^{3+} is important in biochemical field. To date, very few molecular receptors have been reported to selectively sense Al^{3+} unlike other metal ions because of its strong hydration ability and specific coordination capability (*20–29*). Conjugates of 1,3-di-derivatized calix[4]arene have been given greater attention owing to their stable cone conformation, easy characterization and easy functionalization to result in requisite size, shape and flexibility to act as specific receptor for ion and or a molecule (*30, 31*). Recently, we have reported the selective recognition of Mg^{2+} by *o*-phenylene-diimine capped conjugate of 1,3-diderivative of calix[4]arene ($\mathbf{C_2}$) (*32*). While exploring the role of the capping moiety in the metal ion recognition,

CONTACT Chebrolu Pulla Rao cprao@iitb.ac.in

the phenylene-diimine moiety in C_2 was replaced by cyclohexane-diimine to result in **L**. Such variation in the capping moiety brought a huge difference in the selectivity of the receptor from Mg^{2+} to Al^{3+} on going from $\mathbf{C_2}$ to **L**. Therefore, in the present paper, calix[4]arene 1,3-di derivatized cyclohexane-1,2-diimine capped derivative (**L**) has been synthesized, characterized and its sensing ability towards Al^{3+} has been demonstrated by absorption and emission spectroscopy and the binding was proven by ITC, and the bound species were identified by ESI MS and its structural features by DFT computations. The induced microstructural features of **L** by Al^{3+} were probed by scanning electron microscopy (SEM). The suitability of **L** in sensing Al^{3+} salt in powder form was shown by fluorescence microscopy.

Experimental details

Absorption and fluorescence titrations

The bulk solutions of **L** and the salts possessing the requisite cation have been prepared in acetonitrile at 6×10^{-4} M. All the fluorescence titrations were carried out at λ_{ex} = 380 nm on Perkin Elmer LS55 using slit widths of 5 nm and a scan speed of 200 nm/min. Absorption studies have been carried out on JASCO V-570 using the same solutions. All the fluorescence and absorption titrations have been carried out in 1 cm quartz cells by maintaining the final [**L**] of 5 μM prepared in a total volume of 3 mL achieved by diluting with requisite volume of acetonitrile.

Calorimetric titrations

The calorimetric titrations have been performed at 20 °C with a MicroCal ITC 200 isothermal titration calorimeter procured from MicroCal (Northampton, MA, USA). A 40 μL of Al^{3+} of 5 mM solution in syringe has been added to the ligand **L** of 0.5 mM in the cell by means of twenty injections. The first addition contains 0.2 μL and the successive additions of 2 μL of Al^{3+} has been given by maintaining a time spacing of 150 s between each injection. The ITC data were fitted with origin software package provided by MicroCal by using One Set of Sites curve fitting model. Each time a control experiment is carried out without taking **L**, and the corresponding data is subtracted from the main titration data and the resultant one is subjected to the curve fitting.

Sample preparation for SEM

For SEM studies, 40 μL aliquots of **L** (5 μM) and {**L** + Al^{3+}}, in acetonitrile were sonicated for 15 min and the samples were drop casted on aluminium surface and were dried under IR lamp.

DFT computational optimization study

The initial structures of **L** were generated using Gaussview (*33*) from experiment to computational approach and the computations were carried out using the Gaussion 09 package (*34*). Each of the *tert*-butyl moiety present in this structure (*35*) was replaced by hydrogen and thus the corresponding de-tertiarybutylated version, i.e. $\mathbf{L_{DFT}}$ was optimized at PM6 level of theory. In the calculations, both the salicyl-OH groups were deprotonated from $\mathbf{L_{DFT}}$ and generated its dianionic form, *viz.*, $\mathbf{L_{DFT}}^{2-}$. Both the dianionic form and its complex with Al^{3+} were subjected to computational study. The metal ion, Al^{3+} was placed at the vicinity of the binding arms of the $\mathbf{L_{DFT}}^{2-}$ and subjected to PM6 minimization. The output of the metal complex, *viz.*, {$\mathbf{L_{DFT}}^{2-}$ + Al^{3+}} from PM6 optimization was utilized as initial input for the DFT and were further optimized at MO6L level of theory using 6–31G(d,p) basis set.

Synthesis and characterization of L

The synthesis of all the precursors ($\mathbf{P_1}$, $\mathbf{P_2}$ and **L'**) (Scheme 1) has been reported by us recently (*35*) and their

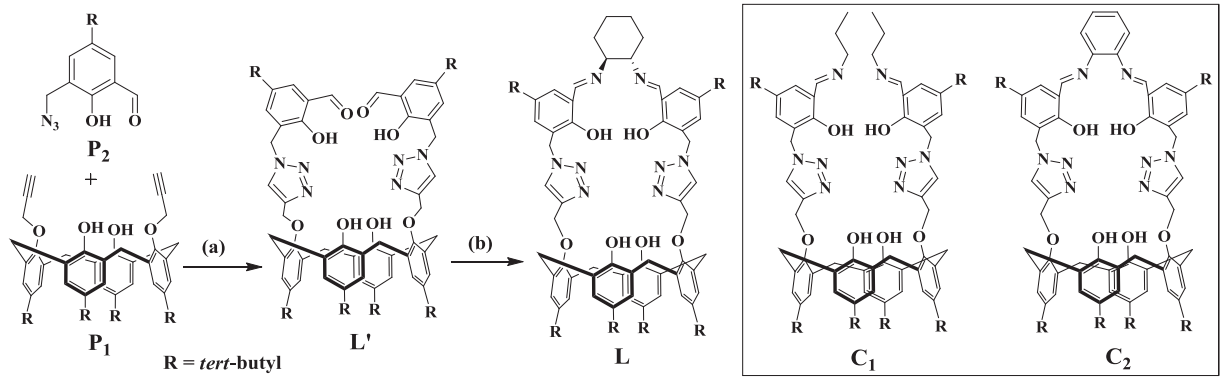

Scheme 1. Synthesis of **L**: (a) $CuSO_4.5H_2O$, soduim ascorbate, dichloromethane: water (1:1), rt, 12 h; (b) *trans*-1, 2-diamino-cyclohexane, CH_3OH, rt, 12 h. The box shows the schematic structures of two control molecules, *viz.*, $\mathbf{C_1}$ and $\mathbf{C_2}$.

characterization data has been given in the supporting information (SI01). The compound **L′** (1.00 g, 0.839 mmol) was dissolved in 20 mL of methanol by heating. To this, *trans*-1,2-diamino-cyclohexane (0.09 g, 0.839 mmol) was added wherein the colourless solution turns to yellow immediately and the solution was stirred for 12 h at RT. The yellow precipitate obtained was filtered and washed with methanol 4–5 times and was dried under vacuum to afford pure product of **L** (0.8 g) in 74% yield. **^{1}H NMR ($CDCl_3$, δ ppm)** 13.7 (broad s, 2H, Sal-O**H**), 8.1 (s, 2H, Sal-imine-**H**), 7.9 (s, 2H, triazole-**H**), 7.03–7.32 (m Ar–**H**), 7.01 (s, 2H, Ar-O**H**), 6.9 (s, 4H, Ar–**H**), 6.7 (s, 4H, Ar–**H**),,5.4–5.5 (m, 4H, Sal-C$\mathbf{H}_2$), 5.1–5.2 (m, 4H, Ar-OC$\mathbf{H}_2$), 4.1–4.2 (m, 4H, Ar-C$\mathbf{H}_2$-Ar), 3.1–3.2 (m, 4H, Ar-C$\mathbf{H}_2$-Ar), 1.8–1.4, 1.2, 0.9 (m, cyclohexane-C$\mathbf{H}_2$), 1.24 (s,18 H, -C(C$\mathbf{H}_3$)$_3$), 1.16 (s, Ar-C(C$\mathbf{H}_3$)$_3$), 0.96(s, 18 H, Ar-(C$\mathbf{H}_3$)$_3$); ^{13}C NMR ($CDCl_3$, (δ ppm): 165.1, 157.3, 150.6, 149.6, 147.3, 144.2, 141.7, 141.4, 132.8, 132.7, 132.6, 130.6, 129.0, 128.2, 127.9, 127.8, 125.8, 125.7, 125.2, 124.2, 122.06, 118.3, 72.5, 70.3, 49.1, 34.1, 34.0, 33.9, 31.8, 31.5, 31.2, 24.3; **HRMS**: for $C_{80}H_{100}O_6N_8$ $[M + K^+]^+$ calculated: 1269.7844, found: 1269.7852. Elemental Analysis: For $C_{81}H_{102}Cl_2N_8O_6$ (**L** + CH_2Cl_2) Calculated: C = 71.82%, H = 7.59%, N = 8.27%; Observed: C = 71.90%, H = 7.60%, N = 8.44%. All the spectra and the elemental data report for **L** are given under the supporting information, SI01.

Results and discussions

The prime purpose to synthesize and study the recognition behavior of **L** is to understand the effect of the capped moiety in calix[4]arene on the ion selectivity. The **L** possesses non-aromatic cyclic ring in the cap in place of a rigid aromatic ring that was present in case of **C_2**. Such structural variation from a rigid aromatic ring to flexible non-aromatic ring is expected to bring in some changes in its ion selectivity preference. The **L** was synthesized in four steps (Scheme 1) starting from *p-tert*-butylcalix[4] arene which includes the synthesis of the precursors **P_1** and **P_2**. The product at every stage was well characterized by ^{1}H, ^{13}C-NMR and ESI-MS, and the purity was confirmed by elemental analysis (SI01). Based on the studies presented in this paper, the **L** showed preference towards Al^{3+} over Mg^{2+} while the latter was preferred when fixed planar aromatic moiety was present as capping moiety, as in **C_2** (*32*). Therefore, the conjugate **L** has been subjected to the interaction study with different metal ions including Al^{3+} and Mg^{2+}.

Al^{3+} ion sensing of L by spectroscopy

The interaction studies of **L** have been addressed by measuring the fluorescence spectra using the metal ions, such as, Mg^{2+}, Zn^{2+}, Cu^{2+}, Ni^{2+}, Ca^{2+}, Fe^{2+}, Mn^{2+}, Co^{2+}, Pb^{2+}, Cd^{2+}, Fe^{3+}, K^+, Na^+, Ag^+, Hg^{2+} and Al^{3+} (SI02). The ligand, **L** is a weak emitter at ~445 nm upon exciting at 380 nm as its fluorescence emission is quenched due to the photoelectron transfer (PET) from the lone pair of nitrogen to the salicylaldimine moiety. Increase in the fluorescence intensity was observed when **L** was titrated with Al^{3+} as a result of ion binding to **L** (Figure 1(a)). The intensity vs. [Al^{3+}]/[**L**] plot for the emission band at 445 nm shows ~45-fold increase in the intensity (Figure 1(c)) which is attributable to the reversal of PET upon the binding of Al^{3+} to the capped iminophenolic core of **L**. The binding is associated with a K_a of $(1.2 \pm 0.3) \times 10^4$ M^{-1} as calculated from the fluorescence data using Benesi-Hildebrand equation (SI03). Fluorescence titration of **L** with Al^{3+} exhibited a lowest detection limit of 9 μM (234 ± 20 ppb).

In order to check whether the Mg^{2+} binds to **L**, the corresponding fluorescence titration was carried out and observed only a marginal enhancement (~3-fold) in the emission intensity (Figure 1(b), SI02) supporting that the receptor **L** is non-selective for Mg^{2+}. This means that the alteration of the capped moiety from phenylene-diimine to cyclohexyl-diimine, resulted in a significant change in the sensitivity of the calix[4]arene conjugate and the selectivity changes from Mg^{2+} to Al^{3+} on going from **C_2** to **L**. The fluorescence titrations were further extended

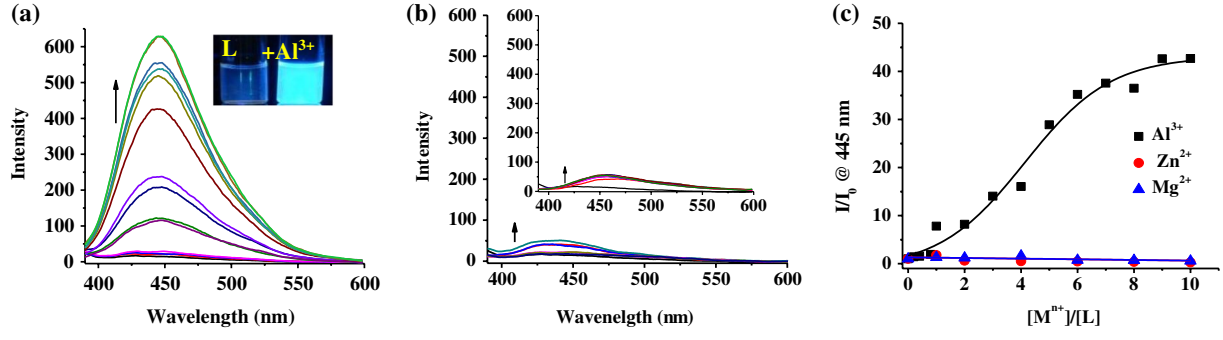

Figure 1. Fluorescence titration of **L** with M^{n+} in acetonitrile (λ_{ex} = 380 nm): Spectral traces of titration with (a) Al^{3+} {Inset = visual color of the solutions of **L** with Al^{3+} observed under UV lamp} (b) Mg^{2+} and inset is for Zn^{2+}. (c) Relative intensity vs. [M^{n+}]/[**L**] plot.

to different metal ions. Among all other metal ions studied, Zn^{2+} showed only a ~2-fold increase like that of Mg^{2+} in the fluorescence intensity of **L** (Figure 1(b), SI02). No significant change was observed in the emission intensity when titrated with Na^+, K^+, Ag^+, Ca^{2+} and Cd^{2+} salts. On the other hand, the ions such as, Fe^{2+}, Fe^{3+}, Hg^{2+}, Ni^{2+}, Co^{2+} and Mn^{2+} showed fluorescence quenching due to their paramagnetic nature and that of Pb^{2+} due to heavy atom effect (SI02). The selectivity of Al^{3+} has been further studied by carrying out appropriate competitive metal ion fluorescence titrations with {[**L** + Al^{3+}] vs. M^{n+}} (SI04) and found no significant change in the presence of ions, such as, Na^+, K^+, Ca^{2+}, Mg^{2+}, Mn^{2+}, Ni^{2+}, Fe^{2+}, Co^{2+} and Zn^{2+}, suggesting that none of these ions interfere with the sensitivity of Al^{3+} towards **L** (SI04). However, Hg^{2+}, Pb^{2+} and Ag^+ exhibited quenching of fluorescence intensity of the complex, [**L** + Al^{3+}] showing that these ions impair the sensitivity of **L** towards Al^{3+}. This can be qualitatively seen by the visual color change of the solutions under 365 nm light (SI04).

In order to confirm the binding of **L** with Al^{3+}, absorption studies were carried out. The absorption spectrum of **L** exhibits three bands centered at 260, 280 and 330 nm. Upon addition of Al^{3+} to **L**, the absorption spectra exhibited increase in the absorbance at 260 and 280 nm bands, but a decrease in the 330 nm band, while this is shifted to 360 nm (Figure 2(a) and (b)). All the spectral changes resulted in isosbestic points at 265 and 340 nm indicating the binding followed by complexation of Al^{3+} by **L** (Figure 2(a)). The Zn^{2+} and Mg^{2+} showed only marginal changes in the absorbance with no isosbestic points (Figure 2(c)), suggesting that both these ions do not bind strong enough to complex the **L**. In the fluorescence spectral titrations, the Zn^{2+} and Mg^{2+} showed only marginal changes and thus from both the spectral studies, it is concluded that Zn^{2+} and Mg^{2+} do not bind to **L**. Further, both the fluorescence and absorption data supported that **L** is highly sensitive towards Al^{3+} and is selective among all the metal ions studied. The selectivity of **L** towards Al^{3+} was further addressed by comparing this with the titration data of the precursor and or control molecules, such as, **L'**, $\mathbf{C_1}$ and $\mathbf{C_2}$ as given in this paper.

Selectivity determined in comparison with the control molecules

In order to reveal the role of the capped moieties in sensing Al^{3+} by **L**, fluorescence and absorption titrations were carried out with three different control molecules, *viz.*, **L'** (open arms with aldehyde moiety), $\mathbf{C_1}$ (open arms with imine moiety) and $\mathbf{C_2}$ (closed arms with phenylene-diimine core) and the corresponding spectra are given in the supporting information, SI05. The fluorescence titrations of **L'**, $\mathbf{C_1}$ and $\mathbf{C_2}$ with Al^{3+} resulted in ~1.5, ~8 and ~3-fold increase in intensity respectively (Figure 3). The fluorescence enhancement suggests that only the aldehyde core is not suitable enough to bind and exhibit fluorescence enhancement with Al^{3+}. While the imine moiety is suitable for binding, the open arms of imine moieties of $\mathbf{C_1}$ does not provide good binding core and when it is closed with rigid phenylene-diimine as in $\mathbf{C_2}$, the core is not accessible for Al^{3+} interaction and binding, hence only a minimal fluorescence was observed. Similarly, the absorption spectral titrations showed minimal changes in case of **L'** due to aldehyde moiety and marginal changes with isosbestic points in case of $\mathbf{C_1}$ due to the open imine moiety, and however, no change at all in case of $\mathbf{C_2}$ due to the closed rigid phenylene-diimine which does not provide enough access to Al^{3+}. On the other hand, the **L** with closed imine core from a flexible cyclohexyl-diimine is well suited for binding to Al^{3+} by showing ~45-fold of fluorescence intensity and is associated with large changes in the absorption spectra by exhibiting isosbestic points supporting the formation of the complex (Figure 2(a) and (b)). All this yielded selectivity. Thus, the cyclohexyl-diimine cap possesses flexible and appropriate binding core that is suitable for Al^{3+}.

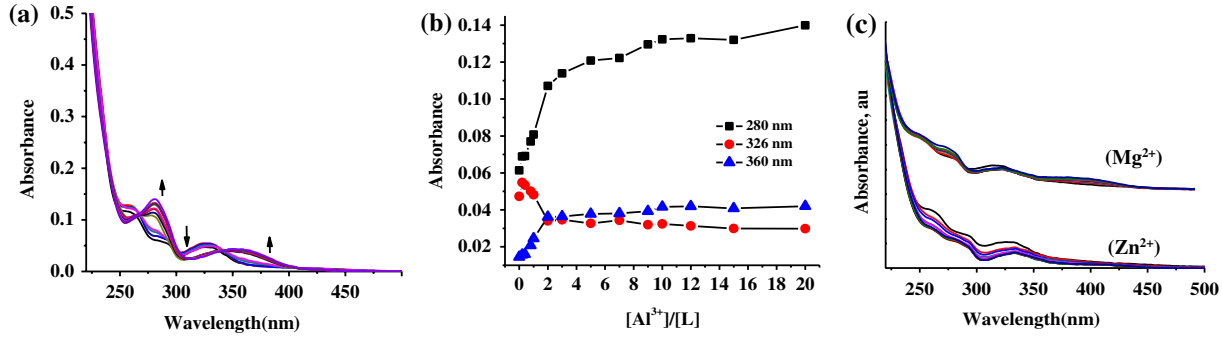

Figure 2. Absorption titration of **L** with metal ions: (a) Spectral traces of the titration with Al^{3+}. (b) Plots of absorbance vs. mole ratio of [Al^{3+}]/[**L**] for different bands. (c) Spectral traces of the titration of **L** with Zn^{2+} and Mg^{2+}.

Binding of Al^{3+} to L by isothermal titration calorimetry (ITC) and the complex by ESI MS

In order to understand and explore the thermodynamic aspects of the binding of Al^{3+} to **L**, isothermal titration calorimetry (ITC) studies have been carried out (Figure 4) as per the details given in the experimental section. The binding of the Al^{3+} gives endothermic thermogram and the heat change observed were almost linear as a function of the mole ratio of Al^{3+} added. The observed data were fitted in 'One Set of Sites' binding model and yielded the stoichiometry of 1:1 between **L** and Al^{3+} with a K_a of $(5.9 \pm 2.0) \times 10^4\ M^{-1}$. In order to confirm the complexation of **L** by Al^{3+}, ESI MS spectra were measured. The **L** shows a molecular ion peak at $m/z = 1269$. In presence of Al^{3+}, a new molecular ion peak was observed at $m/z = 1293.7$ that corresponds to 1:1 complex of Al^{3+} and **L**. The observed isotopic peak pattern for the complex supports the presence of aluminum and this agrees well with the calculated one (Figure 4). When the ESI MS titration was carried out between the control molecules, *viz.*, **L'**, $\mathbf{C_1}$ and $\mathbf{C_2}$, and Al^{3+} (SI06), no peak corresponding to the complex was observed, suggesting that even mass spectrometry reveals that the complex of Al^{3+} is formed only with **L** and not with other control molecules.

Fluorescence microscopy of L and {L + Al^{3+}} in powder

Different ratios of **L** and Al^{3+} were grinded together as their solids and dried under IR lamp. The finely crushed powder of the sample was spread on a glass slide and studied for fluorescence microscopy. The powder **L** alone shows negligible fluorescence intensity (Figure 5(a) and (b)), however, significant fluorescence intensity was observed when 1.3 equiv Al^{3+} salt was powdered with **L** and measured (Figure 5(c) and (d)). The fluorescence microscopy study was extended for the powder samples to the ground mixtures where ~2.5 and ~5.0 equiv of Al^{3+} were added to

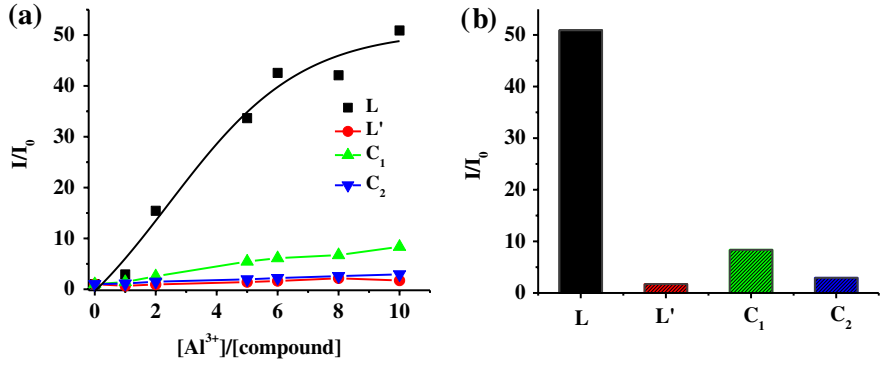

Figure 3. Fluorescence titration of **L**, **L'**, $\mathbf{C_1}$ and $\mathbf{C_2}$ with Al^{3+}: (a) Relative intensity vs. mole ratio plot. (b) Histogram showing relative intensity ratio of different ligands at 10 equivalent addition of Al^{3+}.

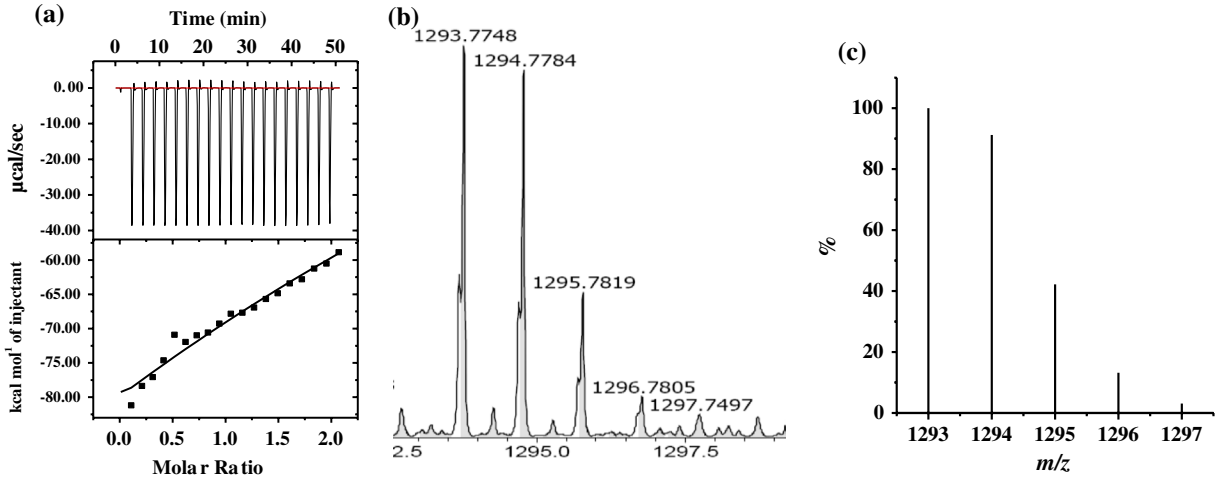

Figure 4. (a) ITC thermogram obtained by the titration of **L** (0.5 mM, in cell) with Al^{3+} (5 mM, in syringe). ESI mass spectral peak for the 1:1 complex of **L** with Al^{3+} along with isotopic peak pattern: (b) observed and (c) calculated.

L. It is observed that the fluorescence intensity of these powder samples increase as the equiv of Al^{3+} increases as shown in Figure 5(e). All these results clearly support that the **L** can sense Al^{3+} in solid state when these two components were ground together.

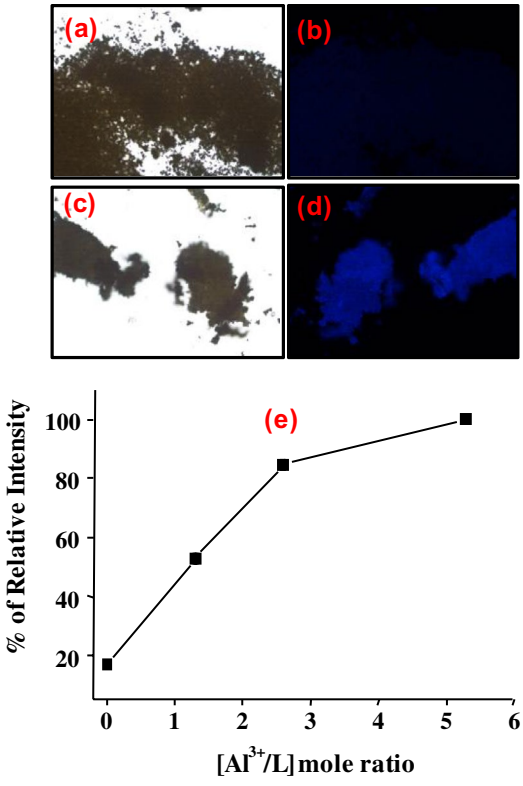

Figure 5. Fluorescence microscopy of **L** and **L** + Al^{3+} in solid state with ratio of **L** and Al^{3+} as 1 : 0 for (a) and (b); 1 : 1.3 for (c) and (d). (a) & (c) are dark field (b) and (d) fluorescence images. (e) Relative intensity vs. [Al^{3+}/**L**] mole ratio plot.

Ion induced supramolecular features in L by scanning electron microscopy

The conjugates of calixarenes are amphiphilic in nature by possessing both hydrophobic and hydrophilic portions together in the same molecule and thus exhibit supramolecular structures through aggregation. In order to explore the aggregational behavior of **L** in presence of Al^{3+}, scanning electron microscopy (SEM) was carried out. The **L** exhibits spherical particles all over the substrate surface (Figure 6(a)–(d)). When Al^{3+} is added to **L**, the spherical particles are transformed into bigger ones to result in micro pots and fibers with sizes ranging from 250 to 900 nm (Figure 6(e)–(h)) supporting that the Al^{3+} induces further aggregation into the supramolecules of **L**.

Structural features of {L_{DFT}^{2-} + Al^{3+}} complex by DFT computations

In order to establish the complexation features of the binding between ligand **L** and Al^{3+}, computational calculations were performed as per the details given under the experimental section. The optimized structure of the dianionic receptor, $\mathbf{L}_{\mathbf{DFT}}^{\mathbf{2-}}$ and its Al^{3+} complex, viz., {$\mathbf{L}_{\mathbf{DFT}}^{\mathbf{2-}}$ + Al^{3+}} are given in Figure 7 and the corresponding coordinate data for the optimized structures is given in the supporting information (SI07 and SI08). In the complex structure, the aluminum center is tetra coordinated to N_2O_2 binding core of the receptor where two nitrogen centers of diimine and two oxygens of salicyl O^- are bound to result in distorted tetrahedral geometry for the metal ion. The corresponding metric data for the coordination core is given in the caption of Figure 7. The bond distances observed in the optimized complex, **{**$\mathbf{L}_{\mathbf{DFT}}^{\mathbf{2-}}$ **+** Al^{3+}**}** indicate strong binding between the metal ion to the receptor in the binding core, and the wide-spread (84.1°–141.6°) and largely deviated

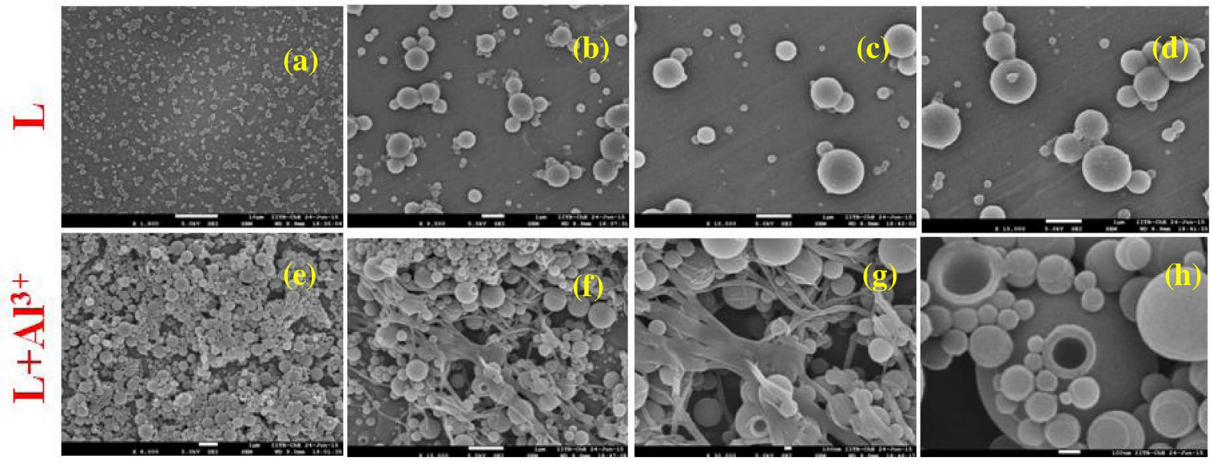

Figure 6. Scanning Electron Microscopy (SEM) images: (a–d) for **L**; (e–h) for {**L** + Al^{3+}}.

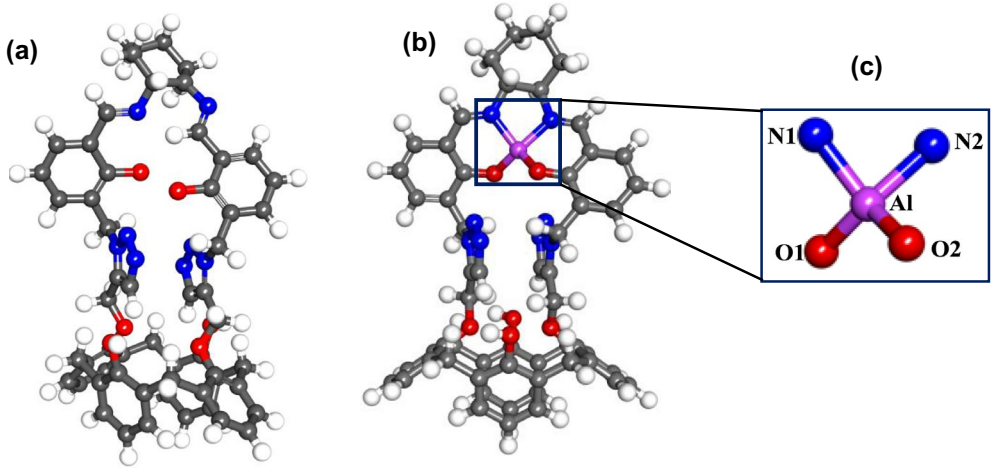

Figure 7. Structures obtained from the optimization carried out at M06L/6-31G(d,p) level of theory: (a) L_{DFT}^{2-} (b) {L_{DFT}^{2-} + Al^{3+}} and (c) is primary coordination for Al^{3+} of complex. Bond lengths and bond angels for the coordination sphere are given in Å and degrees (°): N1–Al = 1.925, N2–Al = 1.921, O1–Al = 1.745, O2–Al = 1.747; N1–Al-N2 = 84.1, N1–Al–O1 = 94.5, N1–Al–O2 = 141.6, N2–Al–O1 = 137.8, N2–Al–O2 = 94.4, O1–Al–O2 = 111.0.

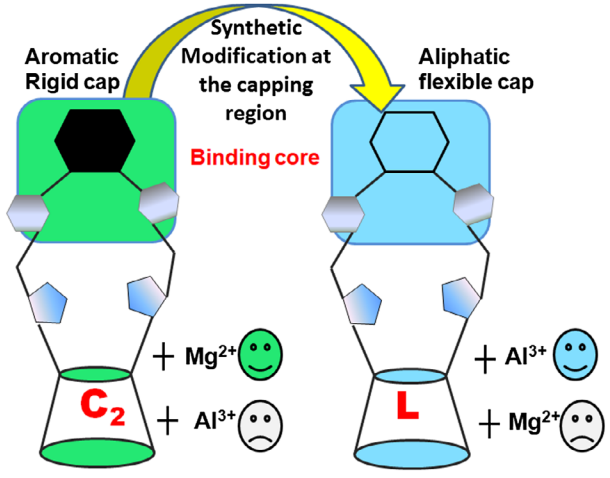

Scheme 2. Schematic representation of the differential behaviour of sensing of Mg^{2+} vs. Al^{3+} by changing the aromatic rigid cap (C_2) to aliphatic-cyclic flexible cap (**L**) on 1,3-di-calix[4]arene.

bond angles of the primary coordination sphere suggest a distorted tetrahedral geometry for the aluminum center.

Conclusions and correlations

In our pursuit to explore the role of the capping moiety on the ion recognition, and in complementing our recent research work (*32*) on the selective recognition of Mg^{2+} by C_2, this paper deals with the impact of the capping moiety on the selectivity of Al^{3+} by the flexible core formed by cyclohexane-1,2-diimine over that of the rigid phenylene-diimine core (Scheme 2). Therefore, a cyclohexane-1,2-diimine capped conjugate of 1,3-calix[4]arene (**L**) was synthesized and thoroughly characterized. The **L** showed ~45-fold enhancement in its emission intensity at 445 nm in presence of Al^{3+}, while exhibited only marginal change in the fluorescence emission intensity in case of Mg^{2+}. Similarly C_2 showed affinity and selectivity only to Mg^{2+} and not to Al^{3+} as reported by us earlier (*32*). Thus, the variation brought in the capping moiety resulted in huge difference in the selectivity of the receptor from Mg^{2+} to Al^{3+} on going from C_2 to **L** as can be noticed from Scheme 2.

All other 15 ions, viz., Mg^{2+}, Zn^{2+}, Cu^{2+}, Ni^{2+}, Ca^{2+}, Fe^{2+}, Mn^{2+}, Co^{2+}, Pb^{2+}, Cd^{2+}, Fe^{3+}, K^{+}, Na^{+}, Ag^{+}, Hg^{2+}, studied were not sensed by **L**. The fluorescence titrations of the precursor and control molecules, viz., **L**′, C_1 and C_2 with Al^{3+} showed no significant changes in the emission intensity suggesting that the capped cyclohexane providing iminophenolic core is essential for the recognition of Al^{3+}. The absorption, ITC and ESI MS supported the complex formation between **L** and Al^{3+}. The fluorescence microcopy results supported that the sensing of Al^{3+} by **L** is feasible in solid state when these are ground together to a fine powder and examined. The Al^{3+} binding induces strong aggregation among **L** and hence the spherical particles of **L** turn to aggregated pot like species supporting that the supramolecular behavior of **L** can be altered by binding of Al^{3+}. For computational ease, each of the *tert*-butyl group present in **L** is replaced by 'H' and the resultant dianionic L_{DFT}^{2-} was optimized. The Al^{3+} complex formed from L_{DFT}^{2-} by computational study yielded a distorted AlN_2O_2 binding core with the receptor molecule where both the imine-N and phenolate-O^{-} bind.

Acknowledgments

CPR acknowledges financial support from the DST/SERB, J. C. Bose National Fellowship and IIT Bombay for Institute Chair Pro-

fessorship. AN & DSY acknowledge UGC for their SRF fellowship. BS gratefully acknowledges the financial support of the Natural Science Foundation of China (Grant No. 21650110464). We thank the FEGSEM central facility of IIT Bombay for providing the service. We thank Dr. Ravinder Kandi for providing the service on fluorescence microscopy for powders.

Funding

This work was supported by DST/SERB [grant number EMR/2014/000985]; J. C. Bose National Fellowship [grant number SB/S2/JCB-066/2015]; Natural Science Foundation of China [grant number 21650110464].

References

(1) Demircelik, A.H.; Andac, M.; Andac, C.A.; Say, R.; Denizli, A. *J. Biomater. Sci.* **2009**, *20*, 1235–1258.
(2) Arduini, M.; Felluga, F.; Mancin, F.; Rossi, P.; Tecilla, P.; Tonellato, U.; Valentinuzzi, N. *Nicola Chem. Commun.* **2003**, 1606–1607.
(3) Sahana, A.; Banerjee, A.; Das, S.; Lohar, S.; Karak, D.; Sarkar, B.; Mukhopadhyay, S.K.; Mukherjee, A.K.; Das, D. *Org. Biomol. Chem.* **2011**, *9*, 5523–5529.
(4) Keawwangchai, T.; Morakot, N.; Wanno, B. *J. Mol. Model.* **2013**, *19*, 1435–1444.
(5) Dong, M.; Dong, Y.M.; Ma, T.H.; Wang, Y.W.; Peng, Y. Inorg. Chim. Acta. 2012, *381*, 137–142.
(6) Maity, D.; Govindaraju, T. *Inorg. Chem.* **2010**, *49*, 7229–7231.
(7) Yu, M.; Yuan, R.; Shi, C.; Zhou, W.; Wei, L.; Li, Z. *Dyes Pigm.* **2013**, *99*, 887–894.
(8) Mu, X.; Qi, L.; Qiao, J.; Ma, H. *Anal. Methods* **2014**, *6*, 6445–6451.
(9) Zhang, K.; Yang, Z.Y.; Wang, B.D.; Sun, S.B.; Li, Y.D.; Li, T.R.; Liu, Z.C.; An, J.M. *Spectrochim Acta A Mol Biomol Spectrosc.* **2014**, *124*, 59–63.
(10) Vallejos, S.; Mu¨noz, A.; Ibeas, S.; Serna, F.; García, F.C.; García, J.M. *J. Hazard. Mater.* **2014**, *276*, 52–57.
(11) Datta, B.K.; Kar, C.; Das, G. *J. Chem. Sci.* **2015**, *127*, 337–342.
(12) Fréry, C.G.; Fréry, N. *EMC – Toxicol. Pathol.* **2004**, *1*, 79–95.
(13) Wang, H.; Zhang, Z.; Sun, A.; Liu, D.; Liu, R. *Talanta* **1996**, *43*, 2067–2072.
(14) Ma, Y.H.; Yuan, R.; Chai, Y.Q.; Liu, X.L. *Mater. Sci. Eng. C* **2010**, *30*, 209–213.
(15) Walton, J.R. *NeuroToxicol.* **2006**, *27*, 385–394.
(16) Polizzi, S. *NeuroToxicol.* **2002**, *23*, 761–774.
(17) Good, P.F.; Olanow, C.W.; Perl, D.P. *Brain Res.* **1992**, *593*, 343–346.
(18) Gupta, V.B.; Anitha, S.; Hegde, M.L.; Zecca, L.; Garruto, R.M.; Ravid, R.; Shankar, S.K.; Stein, R.; Shanmugavelu, P.; Rao, K.S.J. *Cell Mol. Life Sci.*. **2005**, *62*, 143–158.
(19) Perl, D.P.; Gajdusek, D.C.; Garruto, R.M.; Yanagihara, R.T.; Gibbs, C.J. *Science*. **1982**, *217*, 1053–1055.
(20) Chen, C.H.; Liao, D.J.; Wan, C.F.; Wu, A.T. *Analyst*. **2013**, *138*, 2527–2530.
(21) Ma, T.H.; Dong, M.; Dong, Y.M.; Wang, Y.W.; Peng, Y. *Chem. Eur. J.* **2010**, *16*, 10313–10318.
(22) Maity, D.; Govindaraju, T. *Chem. Commun.* **2010**, *46*, 4499–4501.
(23) Samanta, S.; Goswami, S.; Hoque, M.N.; Ramesh, A.; Das, G. *Chem. Commun.* **2014**, *50*, 11833–11836.
(24) Sarkar, D.; Pramanik, A.; Biswas, S.; Karmakar, P.; Mondal, T.K. *RSC Adv.* **2014**, *4*, 30666–30672.
(25) Wang, J.; Pang, Y. *RSC Adv.* **2014**, *4*, 5845–5848.
(26) Wang, Y.W.; Yu, M.X.; Yu, Y.H.; Bai, Z.P.; Shen, Z.; Li, F.Y.; You, X.Z. *Tetrahedron Lett.* **2009**, *50*, 6169–6172.
(27) Velmurugan, K.; Mathankumar, S.; Santoshkumar, S.; Amudha, S.; Nandhakumar, R. *Spectrochim Acta A Mol Biomol Spectrosc.* **2015**, *139*, 119–123.
(28) Kim, K.B.; You, D.M.; Jeon, J.H.; Yeon, Y.H.; Kim, J.H.; Kim, C. *Tetrahedron Lett.* **2014**, *55*, 1347–1352.
(29) Jeyanthi, D.; Iniya, M.; Krishnaveni, K.; Chellappa, D. *RSC Adv.* **2013**, *3*, 20984–20989.
(30) Joseph, R.; Rao, C.P. *Chem. Rev.* **2011**, *111*, 4658.
(31) Acharya, A.; Samanta, K.; Rao, C. P. *Coord. Chem. Rev.* **2012**, *256*, 2096–2125.
(32) Nehra, A.; Hinge, V.K.; Rao, C.P. *J. Org. Chem.* **2014**, *79*, 5763–5770.
(33) Nielsen, A.B.; Holder, A.J. *Gauss View 5.0*, User's Reference; GAUSSIAN Inc.: Pittsburgh, PA, **2009**.
(34) Frisch, M.J.; Trucks, G.W.; Schlegel; H.B.; Scuseria, G.E.; Robb, M.A.; Cheeseman, J.R; Scalmani, G.; Barone, V.; Mennucci, B.; Petersson, G.A.; Nakatsuji, H.; Caricato, M.; Li, X.; Hratchian, H.P; Izmaylov, A.F.; Bloino, J.; Zheng, G.; Sonnenberg, JL.; Hada, M.; Ehara, M.; Toyota, K.; Fukuda, R.; Hasegawa, J.; Ishida, M.; Nakajima, T.; Honda, Y.; Kitao, O.; Nakai, H.; Vreven, T.; Montgomery, J.A., Jr.; Peralta, J.E.; Ogliaro, F.; Bearpark, M.; Heyd, J.J.; Brothers, E.; Kudin, K.N.; Staroverov, V.N.; Kobayashi, R.; Normand, J.; Ra-ghavachari, K.; Rendell, A.; Burant, J.C.; Iyengar, S.S.; Tomasi, J.; Cossi, M.; Rega, N.; Millam, J.M.; Klene, M.; Knox, J.E.; Cross, J.B.; Bakken, V.; Adamo, C.; Jaramillo, J.; Gomperts, R.; Stratmann, R.E.; Yazyev, O.; Austin, A.J.; Cammi, R.; Pomelli, C.; Ochterski, J.W.; Martin, R.L.; Morokuma, K.; Zakrzewski, V.G, Voth, G.A.; Salvador, P.; Dannenberg, J.J.; Dapprich, S.; Daniels, A.D.; Farkas, O.; Foresman, J.B.; Ortiz, J.V.; Cioslowski, J.; Fox, D.J. Gaussian, Inc.: Wallingford CT, **2009**.
(35) Pathak, R.K.; Dikundwar, A.G.; Row, T.N.G.; Rao, C.P. *Chem. Commun.* **2010**, *46*, 4345–4347.